results obtained with this method for two microstrip antennas. These results are compared with measurements realised using the well known gain comparison technique. The discrepancy is ~0·2 dB at the central frequency. Fig. 2 shows the experimental graph of the function g, obtained for the first microstrip antenna array. The value found for $1/G$ is 0·0362 at the central frequency. It gives $G = 14{\cdot}41$ dB. Tables 2 and 3 give results obtained for pyramidal horns and compare them with manufacturer specified gains. The difference is ~0·4 dB at the central frequency.

Table 2 RESULTS OBTAINED FOR PYRAMIDAL HORN IN Ka BAND WITH 1 GHz FREQUENCY SWEEPING

Centre frequency	x	Number of oscillations	Gain with presented method	Manufacturer specified gain
GHz	cm		dB	dB
28	45	3	19·7	19·3
32	45	3	20·2	19·85
35	45	3	20·3	20·3
38	60	4	20·6	20·8

Table 3 RESULTS OBTAINED FOR TWO PYRAMIDAL HORNS IN W BAND WITH 2 GHz FREQUENCY SWEEPING

Centre frequency	x	Number of oscillations	Gain with presented method	Manufacturer specified gain
GHz	cm		dB	dB
94	15	2	19·9	20
94	30	4	20·8	21

Conclusion: We have proposed an automatic method of gain measurement which replaces the tedious mechanical displacement by simple frequency sweeping. The antenna gain obtained by this method has good precision if an appropriate choice of the frequency sweep range and of the reflecting plane position is made. Furthermore the method becomes very attractive for gain measurements at high frequencies.

8th May 1992

Ph. Coquet, K. Mahdjoubi and C. Terret (*Antennas and Microelectronics Laboratory, URA No. 834—CNRS, Université de Rennes 1, 35042 Rennes Cédex, France*)

References

1 SILVER, S.: 'Microwave antenna theory and design' (McGraw-Hill, New York, 1949), pp. 581–592
2 PIPPARD, A. B., BURRELL, O. J., and CROMIE, E. E.: 'The influence of re-radiation on measurements of the power gain of an aerial', *J. IEE*, 1946, **93**, (3A), pp. 720–722
3 WU, Z.: 'Effect of mismatch on antenna gain measurement by Purcell's method', *Electron. Lett.*, 1986, **22**, pp. 522–524
4 LEE, R. Q., and BADDOUR, M. F.: 'Absolute gain measurement of microstrip antennas under mismatched conditions', *Electron. Lett.*, 1988, **24**, pp. 521–522
5 MOTTA CRUZ, E., and DANIEL, J. P.: 'Experimental analysis of corner-fed printed square patch antennas', *Electron. Lett.*, 1991, **27**, (16), pp. 1410–1412

NOVEL VERTICAL DIRECTIONAL COUPLER MADE BY FIELD-ASSISTED ION-EXCHANGED SLAB WAVEGUIDES IN GLASS

P. C. Noutsios, G. L. Yip and J. Albert

Indexing terms: Directional couplers, Optical couplers, Optical waveguides, Integrated optics

Novel vertical directional couplers, consisting of graded-index planar waveguides, were realised by field-assisted K^+-ion exchange in glass. Normal mode measurements of the coupling length are compared to results based on numerical simulations of the diffusion equation and the beam propagation method.

Introduction: Passive waveguide components fabricated by K^+–Na^+ ion-exchange in glass have demonstrated high potential for applications in low-loss singlemode integrated optical devices. Recently, active components made by combining these ion-exchanged guides with overlayers of semiconductor have received considerable attention for optical detection applications [1]. In this waveguide-photodetector geometry, singlemode surface guides are used to increase the coupling efficiency of the guided wave to the detector. However, these waveguides are not adequate for efficient fibre-guide coupling with a minimal insertion loss. An improved configuration would call for fibre coupling to a buried waveguide which can transfer almost all the power to a surface guide through a vertical directional coupler, as shown in Fig. 1. Recently, we reported the successful realisation of such vertical couplers made by field-assisted K^+-ion exchange in glass [2]. This Letter describes the fabrication, measurement and numerical modelling of such a device based on the graded-index (GRIN) profiles of the coupler and the beam propagation method.

Fabrication and measurement: This vertical coupler, comprising two parallel slab waveguides, is fabricated by a three-step electric field-assisted K^+-ion exchange in soda-lime glass [3]. The buried guide is made by a two-step exchange, using an applied field of 50 V/mm and exchange time $t_1 = 15$ s in the first step, and 75 V/mm in the second step with time t_2 varying

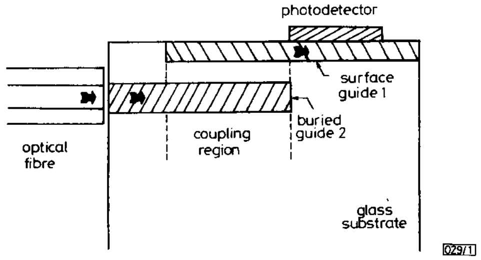

Fig. 1 *Vertical directional coupler used in waveguide-detector geometry*

from 4 to 10 min. The singlemode surface guide is made by a one-step exchange with 50 V/mm applied field and time $t_3 = 5$ s at a constant temperature of 385°C. The TE and TM effective indices of the normal even (N_{even}) and odd (N_{odd}) mode *m*-lines (see Fig. 2*a*) are measured by standard prism coupling techniques at $\lambda_0 = 0{\cdot}633\,\mu m$ with an error of $\pm 2 \times 10^{-4}$. The coupling length L_c can be deduced from the mode-index measurements by [4]

$$L_c = \frac{\pi}{\Delta\beta} = \frac{\lambda_0}{2\,\Delta N_e} \quad (1)$$

where $\Delta N_e = N_{even} - N_{odd}$, $\Delta\beta = k_0\,\Delta N_e$, and $k_0 = 2\pi/\lambda_0$. An input focusing lens is used to excite both modes simultaneously yielding a streak of periodic dots, representing power transfer, on the glass surface as shown in Fig. 2*b*. The period of these dots is equal to twice the coupling length, which was measured carefully for all the fabricated samples and found to be in excellent agreement with measured results according to eqn. 1. In addition, the relative intensities (power ratios) of the normal modes are measured with a vidicon and oscilloscope.

Using the measured ΔN_e and the relative power ratios, the individual mode indices of the surface and buried slabs (N_{e1}, N_{e2}), the coupling coefficient κ, and the power transfer efficiency F can be deduced [4, 5] based on the effective slab configuration of the coupler. The slab indices are found to be

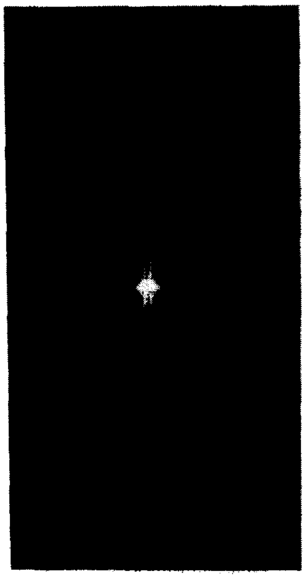

a 029/2

b

Fig. 2 *Output m-lines of even and odd modes and periodic variation of coupled power seen on glass surface*

a Output *m*-lines
b Periodic variation

slightly asynchronous with the difference $N_{e2} - N_{e1}$ being about 2–4 × 10^{-4}. Measurements of the coupling lengths and transfer efficiencies ranged from 200 to 300 μm and 90 to 97%, respectively, for both TE and TM modes. This experimental device already has high values of F, which can be further fine-tuned to yield a good device by a proper design of the input and output sections. Other fabrication conditions can be exploited to make directional couplers with longer coupling lengths and more synchronous slab indices.

Numerical simulations: The GRIN profile of the directional coupler is determined directly from the dopant concentration profile by solving the planar nonlinear ion-exchange equation [6]

$$\frac{\partial c}{\partial t} = \frac{\partial}{\partial x}\left(\frac{D_K}{1 - \alpha c}\frac{\partial c}{\partial x}\right) - \frac{\mu_K E_a^T}{(1 - \alpha c)}\frac{\partial c}{\partial x} \qquad (2)$$

where $\alpha = 0{\cdot}898$ for K^+-ion exchange [7], E_a^T is the total applied electric field, and μ_K, D_K, and $c(x, t)$ are the mobility, selfdiffusion coefficient, and concentration profile of the dopant K^+ ions, respectively. Eqn. 2 is solved by an explicit finite difference scheme. The simulations were carried out by properly adjusting the initial and boundary conditions for each of the three diffusion steps in the total process [8]. Typical GRIN profiles are shown in Fig. 3 for two different exchange times t_2. With $c(x)$ determined, the index profile

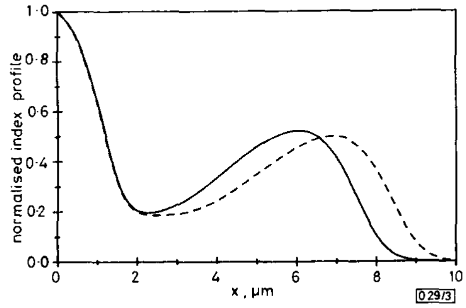

Fig. 3 *Numerical simulations of GRIN profiles of couplers for t_2 = 4·0 min and t_2 = 5·0 min*

——— t_2 = 4·0 min
– – – – t_2 = 5·0 min

$n(x) = n_b + \Delta n_s c(x)$ with $n_b = 1{\cdot}5125$, $\Delta n_s = 0{\cdot}0111$ and 0·0135 for TE and TM modes, respectively [3]. This index profile is then used in the beam propagation method based on the fast-Fourier transform [9] (FFT-BPM) to track the incident wave propagating along the z direction. In our mechanism, the even and odd modes of the coupler are excited at the input simultaneously. However, in the BPM simulation, the incident field launched is assumed to be the fundamental mode of the surface slab guide which is then coupled back and forth between the slabs. The calculated coupling lengths for the TE mode are shown in comparison to the measured ones in Fig. 4, showing very good agreement. Similar agreement is

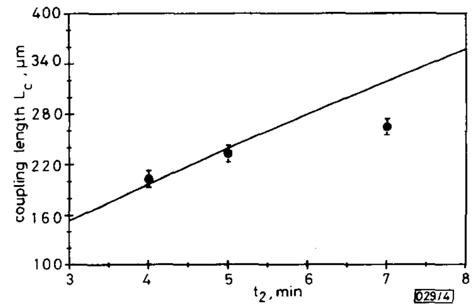

Fig. 4 *Comparison between measured and calculated coupling lengths (TE mode)*

● measured
——— calculated

obtained for the TM mode. In our initial modelling of this device, equivalent step-index (ESI) slab waveguides (equivalent effective index) were constructed and used with the coupled-mode theory to predict the performance [2]. The calculated coupling lengths were about twice as long as the measured ones. This overestimation suggests that the guided field distributions were not adequately accounted for by the ESI model.

Conclusions: The coupling characteristics of a novel vertical directional coupler fabricated by field-assisted ion-exchange in glass are reported. The measured coupling lengths are shown to be in excellent agreement with those computed by the beam propagation method using the numerically modelled graded-index profiles. These couplers can be used as hybrid elements in waveguide-detector geometries on glass substrates with a low insertion loss. Further research is being pursued in the fabrication of couplers with longer coupling lengths and more efficient power transfer.

Acknowledgments: This work was supported by an operating grant and a postgraduate scholarship from the Natural Sciences and Engineering Research Council (NSERC) of Canada and by a contract from the Communications Research Center.

19th May 1992

P. C. Noutsios and G. L. Yip (*Guided-Wave Optics Laboratory, Dept. of Electrical Engineering, McGill University, 3480 University Street, Montreal, Quebec H3A 2A7, Canada*)

J. Albert (*Dept. of Optical Communications Technology, Communications Research Center, 3701 Carling Avenue, Ottawa, Ontario K2H 8S2, Canada*)

References

1 YI-YAN, A., CHAN, W. K., GMITTER, T. J., FLOREZ, L. T., JACKEL, J. L., YABLONOVITCH, E., BHAT, R., and HARBISON, J. P.: 'Grafted GaAs detectors on lithium niobate and glass optical waveguides', *IEEE Photonics Technol. Lett.*, 1989, **1**, pp. 379–380

2 NOUTSIOS, P. C., YIP, G. L., and ALBERT, J.: 'A novel vertical directional coupler made by graded-index ion-exchanged slab waveguides'. Integrated Photonics Research Topical Meeting, New Orleans, 1992, **10**, pp. 156–157

3 YIP, G. L., NOUTSIOS, P. C., and KISHIOKA, K.: 'Characteristics of optical waveguides made by electric-field-assisted K^+-ion exchange in glass', *Opt. Lett.*, 1990, **15**, pp. 789–791

4 NISHIHARA, H., HARUNA, M., and SUHARA, T.: 'Optical integrated circuits' (McGraw-Hill, New York, 1989)

5 MAROM, E., RAMER, O. G., and RUSCHIN, S.: 'Relation between normal-mode and coupled-mode analyses of parallel waveguides', *IEEE J. Quantum Electron.*, 1984, **20**, pp. 1311–1319

6 LILIENHOF, H. J., VOGES, E., RITTER, D., and PANTSCHEW, B.: 'Field-induced index profiles of multimode ion-exchanged strip waveguides', *IEEE J. Quantum Electron.*, 1982, **18**, pp. 1877–1883

7 ALBERT, J., and YIP, G. L.: 'Refractive index profiles of planar waveguides made by ion-exchange in glass', *Appl. Opt.*, 1985, **24**, pp. 3692–3693

8 NOUTSIOS, P. C., and YIP, G. L.: 'Characterization and modeling of planar surface and buried glass waveguides made by field-assisted K^+-ion exchange', to be published in *Appl. Opt.*, 1992

9 NEYER, A., MEVENKAMP, W., THYLEN, L., and LAGERSTROM, B.: 'A beam propagation method analysis of active and passive waveguide crossings', *J. Lightwave Technol.*, 1985, **LT-3**, pp. 635–642

RECEPTION OF FREQUENCY-MODULATED OPTICAL SIGNALS THROUGH INTRACAVITY OPTICAL POWER CHANGE IN INJECTION-LOCKED λ/4-SHIFTED DFB LASER

H. Nakajima, R. Derouiche, J. Charil and P. Correc

Indexing terms: Semiconductor lasers, Photodetectors

A high efficiency optical frequency discriminator/photodetector exhibiting a conversion efficiency exceeding 1 mV/GHz is described. The operating principle consists in monitoring the intracavity optical power change induced by optical FM signals through the voltage change in the phase shifter region of an injection-locked 1·53 μm GaInAs/GaInAsP/InP three-section two-contact λ/4-shifted MQW DFB laser. This principle is demonstrated by demodulating FSK signals at 700 Mbit/s using neither an interferometer nor an additional photodetector. A receiver sensitivity of −21.9 dBm is reported with an NRZ (2^7-1) PRBS.

Introduction: Demodulation of frequency-modulated (FM) optical signals using neither an interferometer nor an additional photodetector has already been demonstrated in a distributed Bragg reflector (DBR) laser amplifier [1], single and two-electrode distributed feedback (DFB) laser amplifiers [2–3] and an injection-locked DFB laser [4–6]. These devices, simultaneously providing spectral selection and recovery of electric signals, are very useful not only for noncoherent densely spaced wavelength division multiplexed (WDM) links but also for compact bidirectional links because frequency shift keyed (FSK) optical signals can also be generated by directly modulating the bias current of a semiconductor laser. As reported previously [4, 5], by monitoring the terminal voltage change induced by the change in the carrier density of an injection-locked laser oscillator, we have demonstrated a demodulation bandwidth exceeding 2 GHz, limited by the bandwidth of the RF amplifier and the locking bandwidth. Because the laser operates at far above the lasing threshold, multigigabit per second operation and a strong suppression of spontaneous emission noise are expected. However, owing to the relatively low efficiencies of conversion from frequency shift to voltage change (~0·2 mV/GHz), which are smaller than those of a conventional demodulation scheme cascading a DFB laser amplifier and a photodetector (~0·6 mV/GHz), the operating bit rate was limited at a few hundred megabits per second.

We report an important improvement of the conversion efficiency by detecting intracavity optical power changes of an injection-locked two contact quarter wavelength shifted multi-quantum well (MQW) DFB laser operating at far above the lasing threshold [7]. By monitoring the voltage change at the phase shifter region, we demonstrate a conversion efficiency exceeding 1 mV/GHz together with a sensitivity of −21·9 dBm at 700 Mbit/s with an NRZ (2^7-1) pseudorandom binary sequence (PRBS).

FM demodulation through intracavity optical power change: In an optically injection-locked single frequency semiconductor laser operating at far above its lasing threshold, the input light induces changes in the intracavity optical power as well as in the forward voltage of the laser [8]. These changes, depending on the frequency detuning ($\delta f = f_i - f_0$, f_i the optical frequency of the input light and f_0 the optical frequency of the receiver laser without injection), result from the carrier-photon relationships involved in any semiconductor laser. In the case of the voltage change provoked by changes in the carrier density, the FM demodulation efficiency (dV/df) is defined as the change in the forward voltage per frequency detuning inside the locking range. Because dV/df is proportional to the derivative of the quasi-Fermi level separation against the carrier density (dV/dN) and is inversely proportional to the linewidth enhancement factor (α) and the differential gain ($\partial G/\partial N$), the efficiency is mainly determined by materials of the active layer and the lasing threshold [5].

The efficiency of conversion associated with the intracavity power can be calculated from the standard rate equations for photons and carriers [9]. In the central region of the locking range, the change in the intracavity power per frequency detuning (dP/df) may be given by the following expression:

$$\frac{dP}{df} = -\frac{4\pi\alpha}{G_N G(1+\alpha^2)}(\gamma_e + \gamma_{eN} + G_N P)$$

where G_N is $\partial G/\partial N$, G is the threshold gain, γ_e is the carrier recombination rate, γ_{eN} is $\partial\gamma_e/\partial N$ and P is the intracavity power. Clearly, the demodulation efficiency associated with the intracavity power change is proportional to the intracavity optical power. This point is very interesting for practical aplications because we can modify the intracavity power by the bias current. Indeed, the intracavity power change may be monitored through the output power by an additional (external) photodiode. It is also monitored by a photodiode placed in the cavity. Of course, by monolithically integrating a photodiode in a DFB laser, a device can be obtained that can act simultaneously as a single frequency laser and a photodiode.

Actually, the device that can perform the detection of the change in the intracavity optical power is a 500 μm long 1·53 μm GaInAs/GaInAsP/InP three-section two-contact λ/4-shifted MQW DFB laser with a grating coupling coefficient (κ) of ~200 cm^{-1} [10]. Both lateral sections are electrically connected together and the centre section playing the role of the phase shifter is separated from the lateral sections. The length of the centre section is ~50 μm. The electrical isolation of the centre section is ~600 Ω. As the laser has a high κL value, the optical field is most likely confined in the centre region of the cavity. Consequently, the intracavity optical power change is the most important in the centre region. The